Regional crustal architecture of Ellesmere Island, Arctic Canada

CHRISTIAN SCHIFFER[1]* & RANDELL STEPHENSON[2]

[1]*Department of Earth Sciences, Durham University, Durham DH1 3LE, UK*

[2]*School of Geosciences, University of Aberdeen, Aberdeen AB24 3UE, UK*

**Correspondence: christian.schiffer@zoho.com*

Abstract: New deep seismological data from Ellesmere Island and the adjacent Arctic continental margin provide new information about the crustal structure of the region. These data were not available for previous regional crustal models. This paper combines and redisplays previously published results – a gravity-derived Moho map and seismological results –to produce new maps of the Moho depth, the depth to basement and the crystalline crustal thickness of Ellesmere Island and contiguous parts of the Arctic Ocean, Greenland and Axel Heiberg Island. Northern Ellesmere Island is underlain by a thick crustal block (Moho at 41 km, *c.* 35 km crust). This block is separated from the Canada–Greenland craton in the south by a WSW–ENE-trending channel of thinned crystalline crust (Moho at 30–35 km, <20 km thick crust), which is overlain by a thick succession of metasedimentary and younger sedimentary rocks (15–20 km). The Sverdrup Basin in the west and the Lincoln Sea in the east interrupt the crustal architecture of central Ellesmere Island, which is interpreted to be more representative of its initial post-Ellesmerian Orogen structure, but with a later Sverdrup Basin and Eurekan overprint.

The Ellesmere Island Lithosphere Experiment (ELLITE), carried out in the framework of the Circum Arctic Lithospheric Evolution (CALE) project, provided the first consistent deep seismological transect for the intra-crustal and Moho structure of the Eurekan Orogen on Ellesmere Island (Fig. 1). These data were published with full documentation in Schiffer *et al.* (2016). The two-dimensional velocity model interpolated by Schiffer *et al.* (2016) between the seven ELLITE stations can be seen in Stephenson *et al.* (2017), where it is integrated with a structural geological cross-section constructed by Piepjohn & von Gosen (2017).

In this paper, the new results, including the implications of the two-dimensional gravity modelling along the ELLITE profile reported by Stephenson *et al.* (2017), are extrapolated across the Eurekan Orogen as a whole, linked with receiver functions from two permanent seismological observatories on Ellesmere Island (Eureka and Alert) and controlled-source seismic observations from the near-offshore of Ellesmere Island. These data are used to construct new maps of the depth to the Moho, using kriging, as well as the depth to the crystalline basement (below what is interpreted as a metasedimentary layer), based on qualitative interpretation, on Ellesmere Island and parts of Axel Heiberg Island. These maps, and their derivative thickness of crystalline crust map, may illuminate the causes and processes of the intraplate crustal deformation in this region.

Tectonic setting

The crust and topography of Ellesmere Island and the surrounding areas were formed by two spatially overlapping, but temporally distinct, orogenic events in the Early Palaeozoic and Palaeogene, with intervening periods of post-Devonian extensional tectonics (Piepjohn *et al.* 2015). The Palaeozoic Ellesmerian orogeny was the Canada–Greenland Arctic equivalent of the Caledonian orogeny in the North Atlantic (Gasser 2013; Gee 2015). The Ellesmerian is characterized by the accretion of shelf-to-deep-water basins and terranes to the Franklinian passive margin of Laurentia under dominantly orthogonal compression (Trettin 1991; Beranek *et al.* 2010; Lawver *et al.* 2011; Lemieux *et al.* 2011; Anfinson *et al.* 2012).

The Sverdrup Basin (Fig. 2) subsided from the Permian until the Palaeogene as a result of extension and/or lithospheric relaxation and collapse of the Ellesmerian Orogen lithosphere (Embry 1991), followed by a period of gradual thermal subsidence (Stephenson *et al.* 1994). The basin is about 1300 km long (NE–SW) and 400 km wide and contains >2 km of Palaeozoic sediments (Davies & Nassichuk 1991) and between 9 and 13 km of Mesozoic–Palaeogene sediments (Embry 1991; Embry & Beauchamp 2008).

Some magmatic rocks were emplaced during the Palaeozoic Ellesmerian orogeny and during the onset of extension related to the opening of the Sverdrup Basin (Embry & Osadetz 1988; Estrada

From: Pease, V. & Coakley, B. (eds) *Circum-Arctic Lithosphere Evolution*. Geological Society, London, Special Publications, **460**, https://doi.org/10.1144/SP460.8

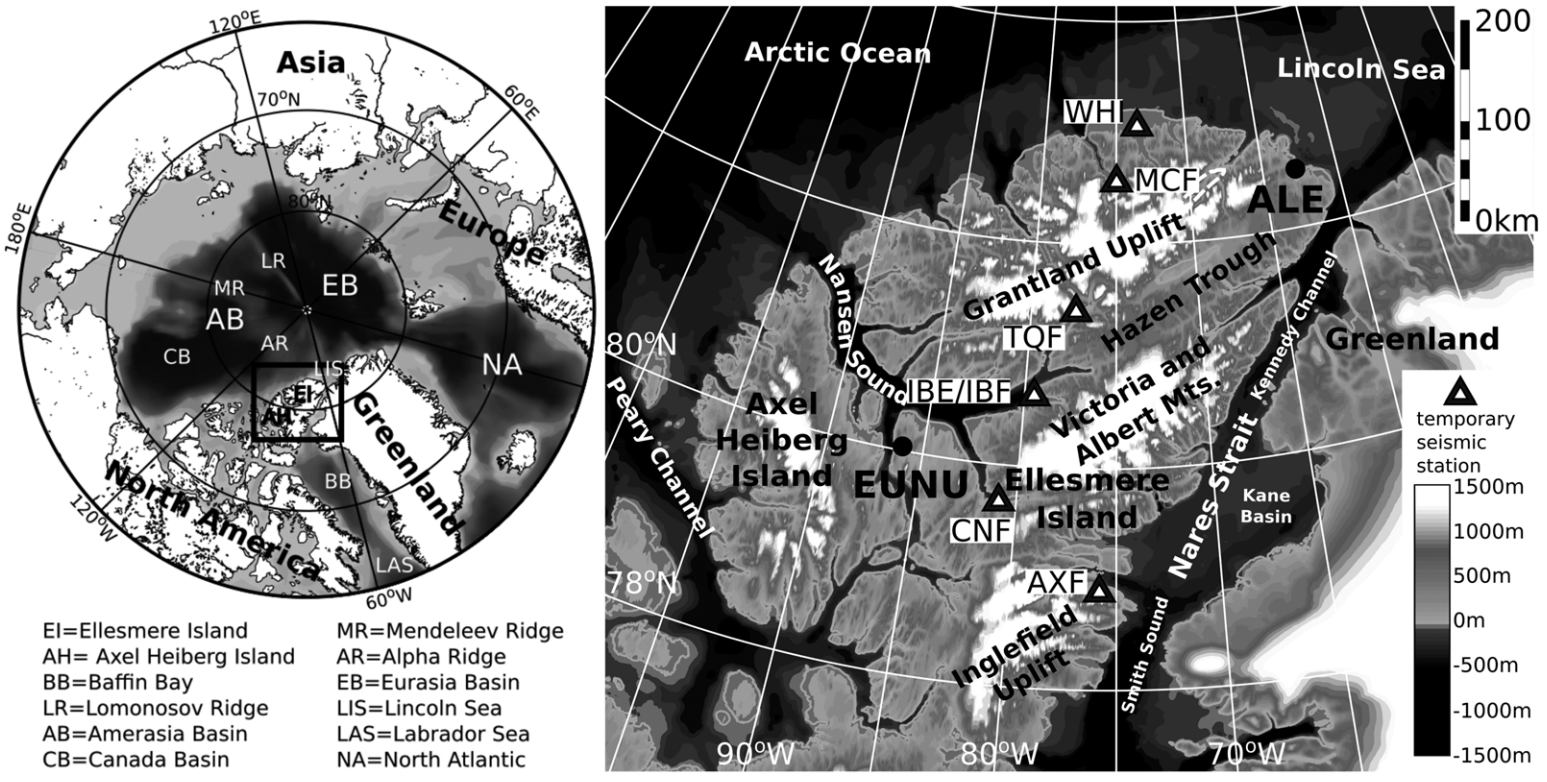

Fig. 1. Maps of the study area. Left panel: location of the study area in a circum-Arctic overview, including bathymetric elements. Right panel: overview map of the study area showing topography (ETOPO1; Amante & Eakins 2009), the ELLITE temporary station positions (triangles), the locations of the Eureka (EUNU) and Alert (ALE) seismic observatories and geographical names.

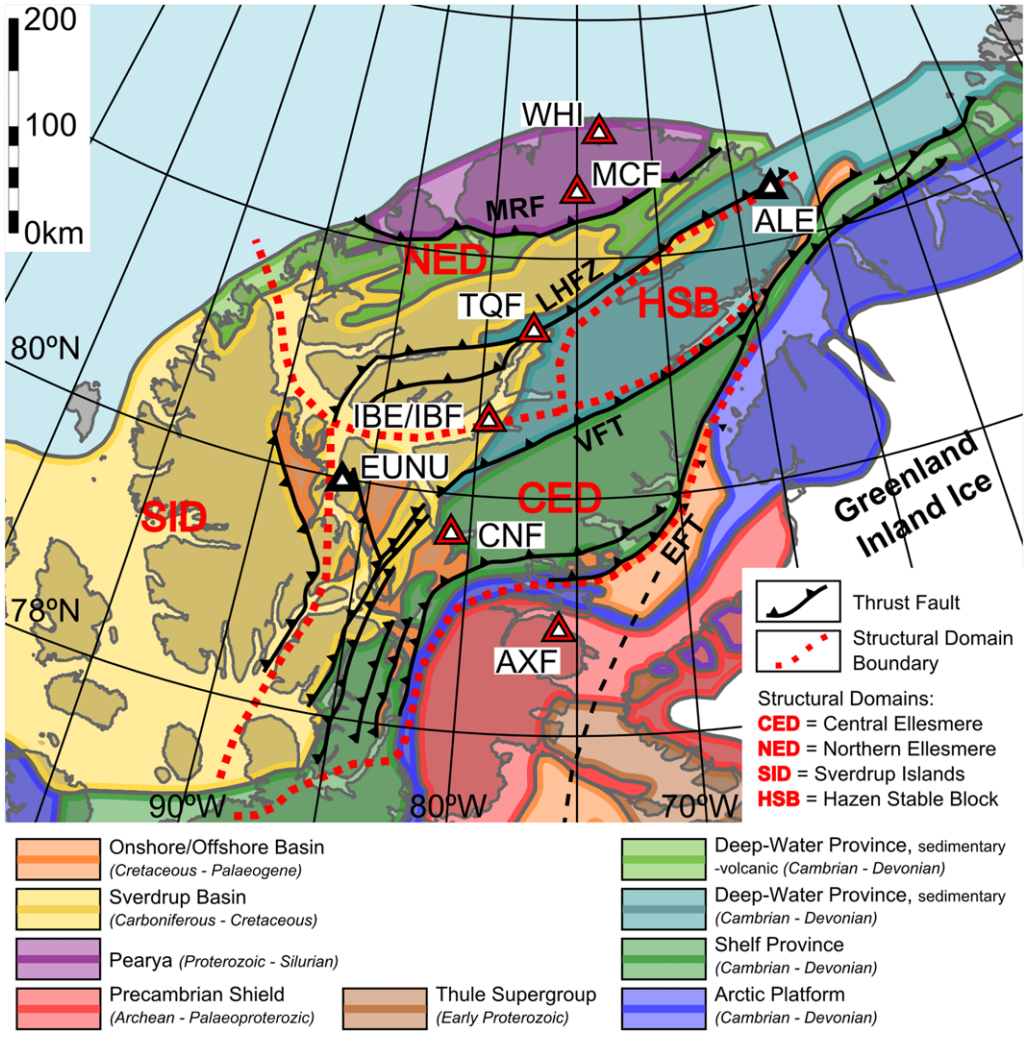

Fig. 2. Geological map of the study area (modified after Oakey & Stephenson 2008). Eurekan structural domains are from Okulitch & Trettin (1991). Faults: EFT, Eurekan Frontal Thrust; LHFZ, Lake Hazen Fault Zone; MRF, Mt Rawlinson Fault; VFT, Vesle Fiord Thrust. Black triangles, permanent stations; red triangles, ELLITE stations.

& Henjes-Kunst 2004; Tegner *et al.* 2011). The largest magmatic event was of Cretaceous–Paleocene age and was associated with the Alpha–Mendeleev Ridge in the adjacent Amerasian segment of the Arctic Ocean (Døssing *et al.* 2013; Pease *et al.* 2014). This onshore–offshore magmatic complex has been referred to as the High Arctic Large Igneous Province (HALIP) (Buchan & Ernst 2006).

Contemporaneous with the emplacement of the HALIP, and possibly linked to it, rifting led to the formation of the Amerasia Basin itself and the present Canadian polar continental margin (Embry 1991; Grantz *et al.* 2011; Døssing *et al.* 2013; Doré *et al.* 2015). The Labrador Sea and Baffin Bay also opened from south to north between Greenland and Canada during the Cretaceous and Palaeogene and into the Eocene (Srivastava 1985; Roest & Srivastava 1989; Oakey & Chalmers 2012; Hosseinpour *et al.* 2013), temporally coincident with a phase of rifting and magmatism in the Lincoln Sea (Døssing *et al.* 2010; Tegner *et al.* 2011). The simultaneous opening of the Labrador Sea–Baffin Bay, the North Atlantic and the Eurasia Basin has been explicitly linked to the anticlockwise rotation of Greenland and, consequently, compression between Ellesmere Island, Greenland and Spitsbergen: the Eurekan orogeny (Tessensohn & Piepjohn

2000; Nielsen *et al.* 2007; Doré *et al.* 2008; Oakey & Chalmers 2012; Gaina *et al.* 2015; Piepjohn *et al.* 2015).

In the Central Ellesmerian Domain (Fig. 2), the structures and deformation are predominantly of Eurekan age, focused along the Eurekan Frontal Thrust, which defines the southern extent of the Eurekan Orogen (Harrison & de Freitas 2007; Piepjohn *et al.* 2015). The Lake Hazen Fault Zone and the Vesle Fiord Thrust are Eurekan-aged structures trending WSW–ENE. Ellesmerian structures were also reactivated during Eurekan orogenesis, particularly in the Northern Ellesmere Domain (Grist & Zentilli 2006; Tessensohn *et al.* 2006; Piepjohn *et al.* 2008, 2015) (Fig. 2), the Lincoln Sea and the Lomonosov Ridge (Døssing *et al.* 2014), but also in the Sverdrup Island Domain (Fig. 2) (Okulitch & Trettin 1991; Harrison 2006). Crustal or lithospheric buckling described in the Sverdrup Island Domain may be linked to Eurekan deformation (Stephenson *et al.* 1990; Stephenson & Ricketts 1990). The Hazen Stable Block (Fig. 2) shows much less Eurekan-aged deformation (Oakey & Stephenson 2008).

Geophysical data

Only one published crustal-scale seismic study in the Sverdrup Basin was available in the study area before the 1990s (Forsyth *et al.* 1979). More wide-angle seismic data were added offshore Axel Heiberg Island (Asudeh *et al.* 1989; Argyle & Forsyth 1994; Forsyth *et al.* 1994, 1998) and in Nares Strait (Reid & Jackson 1997) during the 1990s. Three further studies have since been published, one in the Nares Strait (Funck *et al.* 2006) and two across the Canadian Arctic shelf (Jackson *et al.* 2010; Funck *et al.* 2011).

One permanent seismic observatory (EUNU; Figs 1 & 2) is located at Eureka in the west of Ellesmere Island, installed in the year 2000, and another at Alert (ALE; Figs 1 & 2) in the NW, installed in 1992. Teleseismic receiver functions were recovered and analysed from these observatories, providing estimates of the Moho depth and crustal structure (Dahl-Jensen *et al.* 2003; Darbyshire 2003). From June 2010 to August 2012, seven temporary broadband seismometers comprising the ELLITE array were deployed on a roughly north–south-oriented profile running *c.* 450 km from the Arctic Ocean to the western Kane Basin (Stephenson *et al.* 2013). Receiver functions were recovered and analysed from the ELLITE data as well as from the two permanent stations, adding important information to the crustal structure of previously unsampled areas in the interior of Ellesmere Island (Schiffer *et al.* 2016).

The gravity field of Ellesmere Island has been fully mapped since the late 1980s (Stephenson & Ricketts 1989, 1990; Oakey *et al.* 2001; Oakey & Stephenson 2008). Oakey & Stephenson (2008) published a Moho depth map based on inversion of the compiled gravity grids and topography. This gravity inversion was augmented with some two-dimensional forward modelling on a profile crossing the Eurekan fold–thrust belt in the Central Ellesmerian Domain (Fig. 2) and an analysis of isostatic admittance of the Eurekan Orogen area (Oakey & Stephenson 2008).

The new teleseismic ELLITE data and permanent stations, together with the post-2008 wide-angle seismic studies (Jackson *et al.* 2010; Funck *et al.* 2011), allow an update of the maps of the gravity-derived crustal structure of Ellesmere Island (Oakey & Stephenson 2008), including the Moho depth, the depth to crystalline basement and, from these, the thickness of the crystalline crust.

Crustal cross-sections

Three crustal lithological cross-sections were constructed from the published receiver function data (Schiffer *et al.* 2016) and extrapolated with wide-angle velocity models where feasible (Fig. 3). In these models, the crust is divided into upper, lower and high-velocity lower crust, and the sedimentary layers into soft and consolidated sediments, as well as metasediments. This was based purely on velocity ranges, which are shown in the legend of Figure 4 and described in detail in Schiffer *et al.* (2016). The relationship between lithologies and the seismic data is diffuse, rather than represented as rigidly defined boundaries. Different lithologies may well have similar seismic properties and would fall into the same category (Christensen & Mooney 1995; Christensen 1996; Anderson 2007). This overlap leads to uncertainty in the interpretation of lithology. The V_p and V_s scales in Figure 4 should, accordingly, only be used as a rough guideline. The unconstrained and interpolated areas between the seismic stations are indicated by reduced colour intensity in Figure 4.

Profile 1 (Fig. 4a) is a *c.* north–south-oriented section, including all the ELLITE stations combined with the *c.* 200 km westwards offset wide-angle profile of Funck *et al.* (2011). The topography (Fig. 4a; grey lines on top of the profile; Amante & Eakins 2009) was averaged over different radii (25, 50 and 100 km) on a crooked line following the station locations and then projected onto the section. Although the wide-angle profile is located at some distance, its structure conveniently transitions along-strike into the northern end of the ELLITE section (Fig. 4a; station WHI).

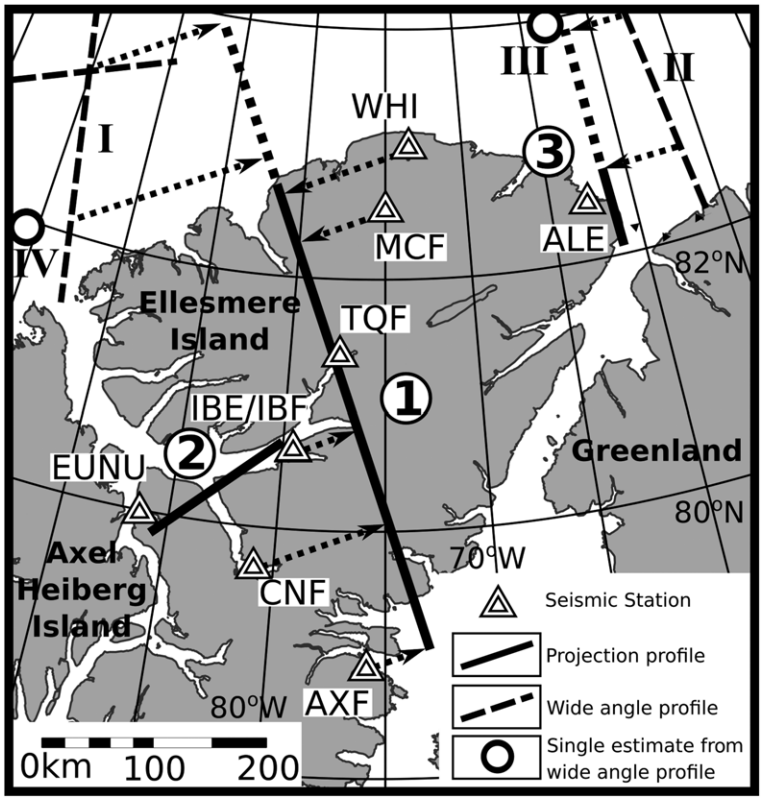

Fig. 3. Overview of the defined crustal cross-sections (profiles 1–3) and the locations of used receiver functions (indicated by three- and four-letter station labels) and wide-angle datasets. Roman numerals: I, Funck *et al.* (2011); II, Jackson *et al.* (2010); III, Forsyth *et al.* (1994); and IV, Argyle & Forsyth (1994).

The lower crust has a similar thickness in both models (*c.* 10 km) and the continental upper–middle crust diminishes in the distal part of the margin, together interpreted as volcanic rocks that may represent oceanic crust. Thick, high-velocity lower crust (*c.* 10 km) is observed in the north of profile 1 on the wide-angle section, where it was interpreted by Funck *et al.* (2011) as magmatic underplating. No lower crustal body is evident to the south on the refraction model, but one does lie in the northern part of the ELLITE section beneath stations WHI and MCF (up to 10 km thick). In the north of the ELLITE profile (stations WHI and MCF), the lower crust is thin (*c.* 7–12 km) and the upper crust is thick (*c.* 15–20 km) beneath a thin (meta-) sedimentary layer (*c.* 5–8 km).

The crust at the southern end of profile 1 in the Greenland–Canada Craton (station AXF) has a similar structure to the northernmost part (thick crystalline crust, thin sedimentary layer). In the interior of Ellesmere Island, the crystalline crust becomes very thin (down to *c.* 18 km), giving way to a thick succession of metasediments (up to 12 km). In the north of the central part of the profile, the upper crust appears to be thicker (*c.* 15 km, although there is a rather large data gap) and in the southern part it appears to be thinner (*c.* 8 km) than the lower crust (6–7 and 10–15 km, respectively).

A greater thickness of unconsolidated sediments, including those of the Sverdrup Basin, are apparent in the Hazen Stable Block (stations TQF and IBE/IBF), where the topography is lowest (Hazen Trough). In the same area, high-velocity lower crust is inferred. Such a high-velocity lower crustal layer is in agreement with the regional gravity field, as shown by Stephenson *et al.* (2017). The highest topography is observed in the Northern Ellesmere Domain (Grantland Mountains), coincident with the thick crust observed in the receiver functions. The topography is also high in the Central Ellesmerian Domain (Victoria and Albert Mountains), where the Moho is deepest (up to 48 km).

Profile 2 (Fig. 4b) was defined between stations EUNU and IBE/IBF and shows the transition from the edge of the Sverdrup Basin in the east (IBE/IBF) to a more central location in the west

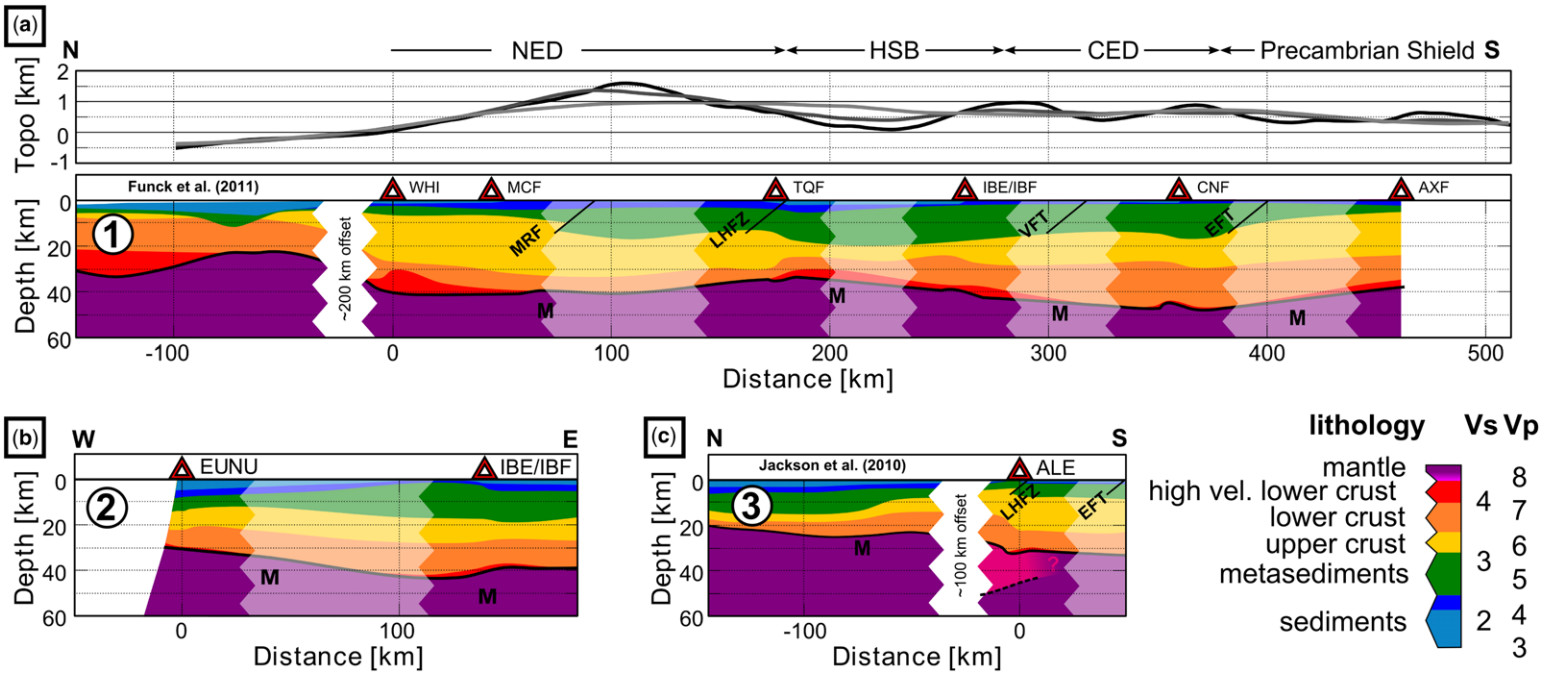

Fig. 4. Schematic crustal cross-sections through Ellesmere Island combining receiver function and wide-angle seismic models. The interpretation of the receiver functions is based on the published velocity model (Schiffer *et al.* 2016, their fig. 10). The colour bar represents the lithological interpretations. Representative V_p and V_s values are shown, which formed the basis of this interpretation. The implied linear relation of V_p, V_s and lithology is much more complex in reality, with overlapping velocity ranges as described in the text. Cross-section locations are shown in Figure 3. The crustal models were interpreted in terms of a sedimentary layer, a metasedimentary layer, upper and lower crust and high-velocity lower crust. (**a**) Profile 1 uses a crustal model from wide-angle seismic data (Funck *et al.* 2011) and all temporary ELLITE stations. The average topography from ETOPO1 (Amante & Eakins 2009) around different radii along the projection line between the stations is shown in the upper panel (dark grey, 25 km; middle grey, 50 km; light grey, 100 km radius). (**b**) Profile 2 is defined between the permanent station EUNU and the ELLITE stations IBE/IBF (west–east), illustrating the deepening Sverdrup Basin. (**c**) Profile 3 is a north–south-oriented section and shows the southern part of a wide-angle seismic model (Jackson *et al.* 2010) combined with the receiver function model at the permanent station ALE. CED, Central Ellesmerian Domain; EFT, Eurekan Frontal Thrust; HSB, Hazen Stable Block; LHFZ, Lake Hazen Fault Zone; M, Moho; MRF, Mount Rawlinson Fault; NED, Northern Ellesmerian Domain; VFT, Vesle Fault Zone. The faults (MRF, LHFZ, VFT, EFT) represent the locations of surface expressions; dip and depth are schematic and not representative.

(EUNU). The crystalline crust is rather uniform in thickness (18–22 km), but the metasedimentary layer thins from the east (*c.* 14 km) to the west (*c.* 5 km). Instead, the overlying sediments of the Sverdrup Basin thicken from <2 km at IBE/IBF to almost 10 km at EUNU.

Profile 3 (Fig. 4c) was defined between the permanent station, ALE, in the NE of Ellesmere Island and the wide-angle profile of Jackson *et al.* (2010), which has <100 km lateral offset to the east from ALE. The crustal structure at ALE and the southern section of the wide-angle model are similar. Upper crust and lower crust each represent *c.* 40–50% of the total depth to the Moho and the metasedimentary layer has a similar thickness in both models (4–6 km, *c.* 10% of the total thickness). The possible north-dipping low-velocity upper mantle structure beneath ALE described by Schiffer *et al.* (2016) is visible beneath ALE, although the robustness of this model element is low (i.e. the receiver function amplitudes are low).

Crustal mapping

The published data described in the preceding sections were collected and combined in new maps of the Moho depth, the depth to the basement and the thickness of the crystalline crust. For the Moho depth, all the seismic constraints presented here were available, as well as the gravity-derived Moho model (Oakey & Stephenson 2008), which allows extrapolation (using kriging) to areas with no seismic data coverage. The receiver function results were augmented by wide-angle data from Jackson *et al.* (2010) and Funck *et al.* (2011), which were sampled every 25 km within the mapping area. The seismic profiles from Argyle & Forsyth (1994) and Forsyth *et al.* (1994) are located just at the edge of the study area and are represented as one data point (III and IV in Fig. 3). The gravity-derived Moho depth (Oakey & Stephenson 2008) was sampled on a grid of 50 km, but not within a radius of 50 km of the seismic observations.

Figure 5a shows the Moho depth estimates of the seismic data on top of the gravity-derived Moho depth model in the study area. The MATLAB kriging toolbox DACE (Lophaven *et al.* 2002) was used to construct the map. For the other two maps, only the seismic constraints were available, why kriging was not used to create the maps, but the surface geology and the tectonic and geological setting allowed substantiated inferences and a qualitative interpretation of the maps. Because the information for the intra-crustal layers is very limited and subject to considerable uncertainty, the interpretation was reduced to only four coarse depth/thickness ranges, which nevertheless illustrates the regional tendencies and trends allowing for large-scale tectonic inferences only. Oakey & Stephenson (2008) presented sedimentary and crustal thickness maps, but the crust included the metasedimentary layer, which is included in the sedimentary package in this study.

Moho depth

A number of additional wide-angle seismic profiles outside the study area are available for comparison, but appear to be generally consistent with the gravity-derived Moho depth model used here (Forsyth *et al.* 1979; Reid & Jackson 1997; Funck *et al.* 2006).

A comparison between the gravity-derived Moho and the newly available seismic data shows the differences and illuminates the importance of the new studies (Fig. 5a), although the differences between the maps resulting from the gridding methodology and data distribution must be taken into consideration. The overall trends and amplitudes in Moho depth are not greatly dissimilar (Fig. 5b). The data show close to the same Moho depth estimates at one station in the north (station MCF) and two stations in the south of Ellesmere Island (stations CNF and AXF), whereas larger discrepancies between the two models are observed at the other locations with receiver functions. At the northernmost station (WHI) the Moho is 5–8 km deeper (*c.* 40–41.5 km) in the seismic estimates than in the gravity model (*c.* 33–35 km). Station ALE (Dahl-Jensen *et al.* 2003; Darbyshire 2003) and the eastern wide-angle profile (Jackson *et al.* 2010) in the Lincoln Sea coastal area show a 5–10 km shallower Moho (*c.* 25–31 km) than the gravity model (*c.* 33–36 km). A shallower Moho, although with a less extreme difference, (*c.* 5 km) is observed along the wide-angle profile in the NW of the study area (Funck *et al.* 2011). The Moho at station EUNU is only 2–4 km shallower in the receiver functions (*c.* 29–31 km) than the gravity model (*c.* 32–34 km). The receiver functions indicate a shallow Moho (*c.* 34–36 km) at station TQF and a deeper Moho (*c.* 38–43 km) at IBE/IBF, whereas the gravity model shows the opposite trend, with a shallower Moho at station TQF (*c.* 36–39 km) and a deeper Moho at station IBE/IBF (*c.* 32–34 km).

Thin crust estimated at station EUNU in the Sverdrup Basin may form a contiguous area of shallow Moho extending northwards to the ocean–continent transition (Funck *et al.* 2011), geographically coincident with the location of Nansen Sound. The gravity model indicated a deep Moho feature (*c.* 35 km) along the northwestern coast of Ellesmere Island, which is not observed in the seismic data. The new data confirm the existence of a 'channel' of shallow Moho in the Hazen Stable Block, although the exact north–south extent

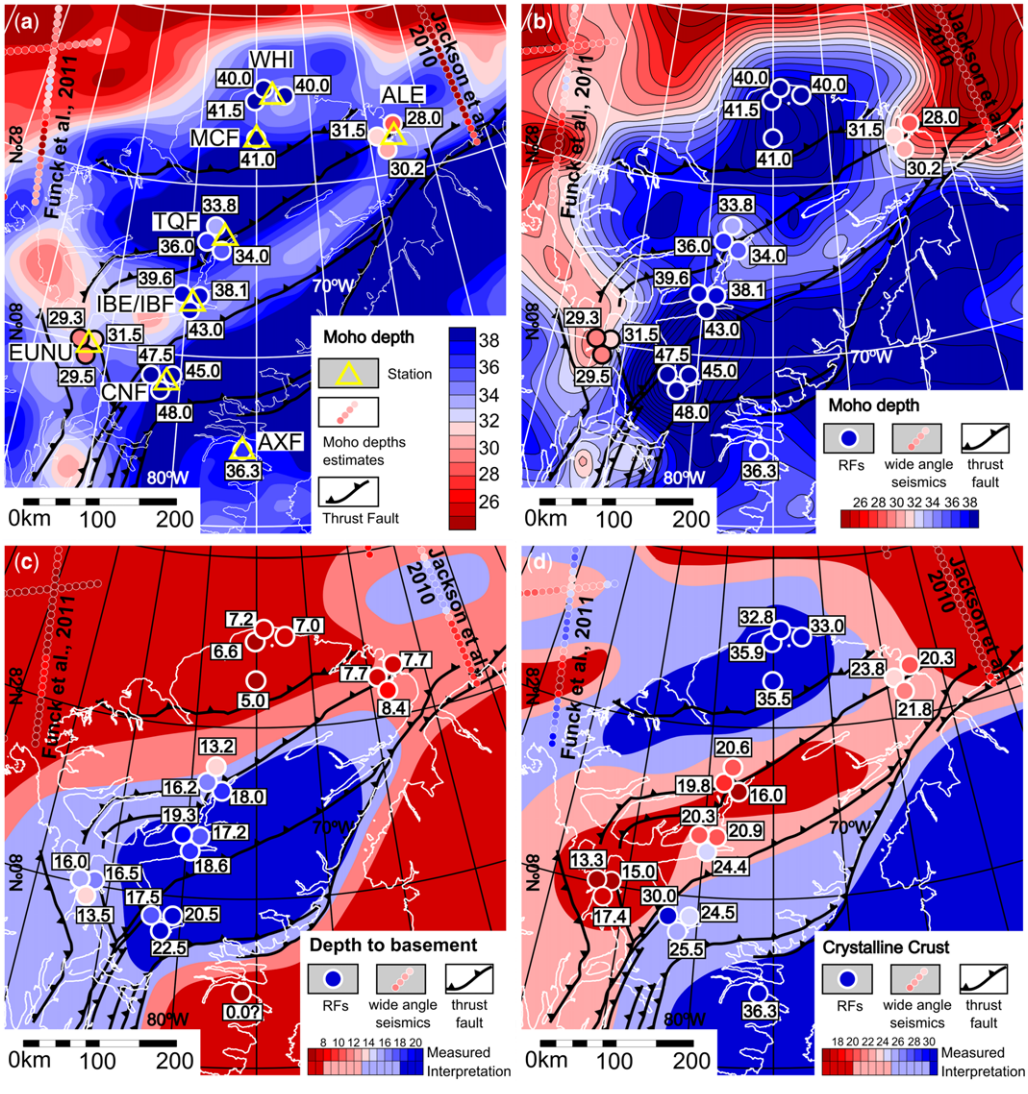

Fig. 5. (**a**) Available deep geophysical data in Ellesmere Island showing where they provide Moho depth constraints. Small circles, wide-angle seismic data; large circles, receiver function data; background, Moho depth from gravity modelling (Oakey & Stephenson 2008); triangles, seismological stations. (b)–(d) New maps. Data in part (b) are shown with the same colour bar as for the observations in part (a), truncated at 24 and 38 km, whereas the black isolines continue to 18 and 48 km, respectively. In parts (c) and (d) a more detailed colour bar is used for the observations ('measured'), whereas the colour bar for the interpretation is reduced to only four depth/thickness ranges because of large uncertainties and few observations (the simplified colour bar 'interpretation'). (**b**) Moho depth derived from kriging of the available geophysical data from receiver functions (large circles), wide-angle seismic data (small circles, sampled at every 25 km) and gravity-derived Moho depth (background, sampled on a 50 × 50 km grid, see text). (**c**) Depth to basement from qualitative interpretation of the available data. (**d**) Thickness of the crystalline crust from qualitative interpretation of the available data. (Large circles- depth estimates from receiver functions. Small circles- depth estimates from wide angle seismics.)

of this channel appears to be different at stations IBE/IBF and TQF. West of station EUNU, the gravity data indicate deepening of the Moho to >32 km, but west of Axel Heiberg Island (outside map boundaries), the Moho is estimated at 26–27 km (Argyle & Forsyth 1994), which could be an expression of crustal buckling or folding (Forsyth *et al.* 1990; Stephenson *et al.* 1990).

Depth to basement

There is little to no seismic constraint for this map on the Canada–Greenland craton, where the sedimentary successions are expected to be thin. One profile from Oakey & Stephenson (2008) includes (meta-)sedimentary layers and indicates a thick sedimentary layer in areas similar to those where the receiver function data suggest it exists, although considerably thinner (9–12 km compared to 16 km). The difference in thickness might be due to uncertainty in the gravity or receiver function modelling and interpretation.

The depth to basement map (Fig. 5c) shows a clear maximum in central Ellesmere Island, confined by the Eurekan Frontal Thrust to the south and the Lake Hazen Fault Zone (see Fig. 2 for location) to the north. The consequent thick sedimentary package mainly consists of metasediments in the central part (stations TCF, IBE/IBF and CNF; see Fig. 5a for locations) and is limited by the Lincoln Sea margin to the NE (station ALE and Jackson *et al.* 2010), where the basement is much shallower (<10 km), implying a thin sedimentary succession. A sedimentary basin of up to 15 km total thickness (up to *c.* 5 km of metasediments) is located in the Lincoln Sea (Jackson *et al.* 2010), where basement depths of *c.* 15 km are observed at shallow water depths. Its lateral extent is not constrained due to a lack of complementary data. To the SW, at station EUNU, the basement is deep at 14–16 km and the metasedimentary succession is inferred to be about 5 km thick (Fig. 4), overlain by younger sediments that make up the Sverdrup Basin succession. The total sedimentary package of the Sverdrup Basin reaches a thickness of >10 km (Embry 1991).

Crystalline basement

The crystalline thickness map (Fig. 5d) was constructed consistently from the difference between the Moho depth and the depth to basement maps and is therefore subject to uncertainties based on previous assumptions, interpretations and extrapolations.

Two areas of thick crystalline crust (>30 km) are observed on Ellesmere Island, one in the north (Pearya) and another in the Canada–Greenland craton south of the Eurekan Frontal Thrust. The thick crust in southern Ellesmere Island coincides with a deep Lithosphere-Asthenosphere-boundary associated with the Canada-Greenland Craton (Schiffer *et al.* 2017). The thick crystalline crust at the two northernmost ELLITE stations (stations WHI and MCF) is limited to the east by thinner crust estimated at station ALE (20–24 km) and the nearby wide-angle profile of Jackson *et al.* (2010) (<20 km); whether this is an abrupt or gradual change cannot be resolved. To the west of stations WHI and MCF, the crystalline crustal thickness decreases to *c.* 26 km at the wide-angle profile of Funck *et al.* (2011). To explain the deep Moho in the absence of any substantial sedimentary succession (<7 km), the area between the southern end of the Funck *et al.* (2011) wide-angle profile and the two northernmost ELLITE stations (WHI and MCF) should have a crustal thickness >30 km.

Thick crystalline crust is also reported at ELLITE station AXF (*c.* 36 km), which is situated at the northern limit of the Canada–Greenland craton. The sedimentary successions for the whole cratonic domain in the study area may be presumed to be absent or very thin. The Proterozoic Thule Supergroup (Dawes 1997) and some offshore basins are located at the southern edge of the study area, but are generally <6 km thick and <2 km thick in the study area (Oakey & Stephenson 2008); accordingly, the thickness of crystalline crust is essentially equivalent to the Moho depth. It follows that the crust must be thicker than 30 km south of the Eurekan Frontal Thrust. Reid & Jackson (1997) estimated a crystalline crustal thickness of 34 km in northern Baffin Bay, just south of the study area.

The Arctic Ocean domain shows a marked difference between the west and east in the study area. Wide-angle models were interpreted to show extremely thick crust (mostly lower crust, including high-velocity bodies) in the west (Funck *et al.* 2011), associated with igneous crust of the Alpha Ridge, whereas in the east the crystalline crust is as thin as *c.* 6–12 km and is covered by thick successions of sedimentary rocks (Jackson *et al.* 2010). The crystalline crust thickens considerably to >25 km further north, outside the study area, towards the Lomonosov Ridge (Jackson *et al.* 2010). Central Ellesmere Island has thin crystalline crust (<25 km) localized along a *c.* 100 km wide WSW–ENE-oriented zone, roughly bounded by the Lake Hazen Fault Zone and the Vesle Fiord Thrust and roughly coincident with the Hazen Stable Block structural domain of the Eurekan Orogen (see Fig. 2 for locations). The central part of this zone shows crystalline crustal thicknesses of <20 km, culminating in a clear minimum at EUNU in the Sverdrup Basin. Wide-angle seismic data west of Axel Heiberg Island (*c.* 200 km west of EUNU, not in the study area) indicate a crystalline crustal thickness of 22 km (Argyle & Forsyth 1994). This indicates a slight increase in crystalline crustal thickness from EUNU across Axel Heiberg Island, as also shown in the gravity model (Oakey & Stephenson 2008).

Tectonic implications

New geophysical data in and around Ellesmere Island add important information to the large-scale

crustal architecture of the region. Some of the most significant differences are seen in the Lincoln Sea region, where the new data indicate the Moho at a much shallower depth than the earlier gravity inversion estimates. The latter may reflect the low-velocity (and probably low-density) uppermost mantle structure observed in the receiver functions at station ALE. The opposite trend is observed in northern Ellesmere Island, where deeper Moho is suggested by the seismic data than by the gravity model. The shallower gravity model Moho may be explained by the very thick high-velocity lower crust observed in the receiver functions. In other regions, the misfit between the gravity and seismic models is smaller, but some minor details are revealed by the new data, allowing for local adjustments of the Moho depth map. The limit of the area of deep Moho (>35 km) is very close to the northern coastline of Greenland and Ellesmere Island. An area of reasonably well-constrained shallow Moho (both by gravity modelling and seismic constraints) coincides with the geographical location of Nansen Sound (see Fig. 1 for location) and suggests a close to local isostatic compensation in the area. This area also approximates the centre of early Cretaceous–Palaeogene magmatism in the Canadian Arctic Islands (Anudu *et al.* 2016; Saumur *et al.* 2016) and it is speculated that the shallow Moho may be related to crustal extension in this area, which is, in turn, linked to the magmatism. It could also be asked whether this eventually had any control over the topographic evolution of Nansen Sound.

The long-wavelength part of the Moho depth map presented here is in general agreement with recent Moho depth models for the entire Arctic region (Lebedeva-Ivanova *et al.* 2015; Petrov *et al.* 2016) and for Greenland (Steffen *et al.* 2017). A slightly better agreement occurs with the Petrov *et al.* (2016) model, which shows two domains of deep Moho in the south and north of Ellesmere Island and the deepest Moho in the Central Ellesmerian Domain (up to *c.* 48 km). The model of Lebedeva-Ivanova *et al.* (2015) also indicates deeper Moho in these regions, but clearly shallower Moho in the latter (<40 km).

A thick (meta-)sedimentary layer is located in the Ellesmerian fold–thrust belt (inferred by the large basement depth), bounded to the north and west by the Lake Hazen Fault Zone and to the south and east by the Eurekan Frontal Thrust (Fig. 5c). These thick metasediments coincide with an elongated zone of thin crystalline crustal thickness, south of which the Canada–Greenland craton is evident, with thick crystalline crust (>35 km). North of the Lake Hazen Fault Zone, a rather well-confined, *c.* 300 × 100 km area of thick crystalline crust is inferred. This area has a close to two-dimensional crustal structure for *c.* 250 km in a WSW–ENE direction along-strike.

This rather uniform crustal architecture terminates at the Lincoln Sea in the NE and the Sverdrup Basin in the SW (Fig. 5). This section may reflect an architecture formed during the Ellesmerian Orogen, with additional crustal shortening and reactivation during the Eurekan orogeny, but less affected by post-Ellesmerian extensional tectonics. By contrast, subsequent extensional episodes have strongly overprinted this original structure to the west, where it is mainly related to Sverdrup Basin extension, and to the east, where it is mainly related to younger transtensional/extensional history related to the Baffin–Arctic–North Atlantic region. The possibility that these two areas of crustal thinning are indicative of ancestral (Ellesmerian) structurally or rheologically different basement types, compared to what is preserved on Ellesmere Island, could also be considered. There is indeed an implication that, if the crustal structure on Ellesmere Island is in part ancestral, then the topography of Ellesmere Island may also be at least partly ancestral.

The zone of shallow Moho in the region of Hazen Stable Block is consistent with a model in which this area was not strongly affected by crustal shortening during the Eurekan orogeny, which is in contrast with clear evidence of crustal thickening and reactivation of Ellesmerian structures in the south and north (Piepjohn *et al.* 2015). Numerical experiments suggest that a lithospheric block in the central part of Ellesmere Island – with a greater strength than in the north and south and the existence of orogenic weaknesses – is able to explain such a deformation and topographic patterns (deformation in the north and south, limited deformation in the centre: the Hazen Stable Block) (Heron *et al.* 2015).

Two areas featuring high-velocity lower crust have been identified. It is speculated that the high-velocity lower crust in Pearya (the Northern Ellesmere Domain) could be linked to the nearby thick, high-velocity lower crust imaged offshore Ellesmere Island by Funck *et al.* (2011), where it has been interpreted as related to Cretaceous–Cenozoic magmatism rather than being an ancestral crustal feature. High-velocity lower crust is also observed in central Ellesmere Island, geographically coincident and possibly related to the shallow Moho observed below the Hazen Stable Block. Two possibilities for its origin are: (1) it is ancestral to the Precambrian-aged Franklinian palaeo-passive continental margin; and (2) it represents a magmatic underplate emplaced during the opening of the Late Palaeozoic origins of the Sverdrup Basin.

Conclusions

We have combined geophysical data, including all the data published since 2008, and compiled new

maps of the Moho depth, the depth to basement and the crystalline crustal thickness for Ellesmere Island and contiguous regions (Fig. 5). Although the Moho generally shows similar patterns and trends to an earlier Moho depth model derived solely from gravity, there are clear local differences (Fig. 5a, b). Shallower Moho (<30 km) is observed close to the Labrador Sea and in the Sverdrup Basin. A WSW–ENE-oriented 'channel' of shallow Moho in the centre of Ellesmere Island (*c.* 81–82° N) is observed in both models, but the new data suggest a slightly different location for this feature. By contrast, the northernmost part of Ellesmere Island has deeper Moho than previously estimated (40–42 km). The depth to basement map (Fig. 5c) shows the deepest basement in the centre of Ellesmere Island (15–20 km), between the Lake Hazen Fault Zone and the Eurekan Frontal Thrust, which follows the general trends of Ellesmerian and subsequent Eurekan deformation. The crystalline crustal thickness map indicates a block of thick crust (30–35 km) in the north of Ellemere Island, separated from the craton in the south by the elongated channel of thinned crust in the Hazen Stable Block (12–20 km) and partly coincident with the inferred thick metasedimentary succession.

The crustal structure (as defined by the Moho depth, the basement depth and the crustal thickness) of central Ellesmere Island probably retains much of what was established during the Palaeozoic Ellesmerian Orogen, but including Eurekan reactivation and deformation in the north and south. To the NE and SW, a substantial change is observed, which interrupts the Eurekan overprinted Ellesmerian orogenic domain of (primarily) Ellesmere Island. In the SW, Late Palaeozoic extension formed the Sverdrup Basin, apparently strongly degrading the original crustal features of the Ellesmerian Orogen. Similarly, local rifting and crustal thinning in the Lincoln Sea may have cut through the older Ellesmerian structure in the Late Cretaceous and early Palaeogene.

The paper was motivated and developed under the umbrella of the project Circum Arctic Lithospheric Evolution (CALE). Thanks are given to the project leaders and all active participants. The paper was produced during a postdoctoral research fellowship of C. Schiffer at Durham University funded by the Carlsberg Foundation. The comments of two anonymous reviewers are much appreciated and have led to a number of important clarifications to our results and interpretations.

References

Amante, C. & Eakins, B.W. 2009. *ETOPO1 1 Arc-Minute Global Relief Model: Procedures, Data Sources and Analysis*. NOAA Technical Mem. NESDIS NGDC-24. NOAA, Silver Spring, https://doi.org/10.7289/V5C8276M

Anderson, D.L. 2007. *New Theory of the Earth*. Cambridge University Press, Cambridge.

Anfinson, O.A., Leier, A.L., Embry, A.F. & Dewing, K. 2012. Detrital zircon geochronology and provenance of the Neoproterozoic to Late Devonian Franklinian Basin, Canadian Arctic Islands. *Geological Society of America Bulletin*, **124**, 415–430, https://doi.org/10.1130/B30503.1

Anudu, G.K., Stephenson, R.A., Macdonald, D.I.M. & Oakey, G.N. 2016. Geological features of the northeastern Canadian Arctic margin (Canada) revealed from analysis of potential field data. *Tectonophysics*, https://doi.org/10.1016/j.tecto.2016.03.025

Argyle, M. & Forsyth, D.A. 1994. *Interpretation of Data and Presentation of Results from the Ice Island 1986 and 1990 Seismic Refraction Experiments*. Geological Survey of Canada Open File Report **2973**, https://doi.org/10.4095/194781

Asudeh, I., Forsyth, D.A., Stephenson, R., Embry, A., Jackson, H.R. & White, D. 1989. Crustal structure of the Canadian polar margin: results of the 1985 seismic refraction survey. *Canadian Journal of Earth Sciences*, **26**, 853–866, https://doi.org/10.1139/e89-069

Beranek, L.P., Mortensen, J.K., Lane, L.S., Allen, T.L., Fraser, T.A., Hadlari, T. & Zantvoort, W.G. 2010. Detrital zircon geochronology of the western Ellesmerian clastic wedge, northwestern Canada: insights on Arctic tectonics and the evolution of the northern Cordilleran miogeocline. *Geological Society of America Bulletin*, **122**, 1899–1911, https://doi.org/10.1130/B30120.1

Buchan, K.L. & Ernst, R.E. 2006. Giant dyke swarms and the reconstruction of the Canadian Arctic islands, Greenland, Svalbard and Franz Josef Land. *In*: Hanski, E., Mertanen, S., Rämö, T. & Vuollo, J. (eds) *Dyke Swarms – Time Markers of Crustal Evolution*. Taylor & Francis, 27–48.

Christensen, N.I. 1996. Poisson's ratio and crustal seismology. *Journal of Geophysical Research: Solid Earth*, **101**, 3139–3156, https://doi.org/10.1029/95JB03446

Christensen, N.I. & Mooney, W.D. 1995. Seismic velocity structure and composition of the continental crust: a global view. *Journal of Geophysical Research: Solid Earth*, **100**, 9761–9788, https://doi.org/10.1029/95JB00259

Dahl-Jensen, T., Larsen, T.B. *et al.* 2003. Depth to Moho in Greenland: receiver-function analysis suggests two Proterozoic blocks in Greenland. *Earth and Planetary Science Letters*, **205**, 379–393, https://doi.org/10.1016/S0012-821X(02)01080-4

Darbyshire, F.A. 2003. Crustal structure across the Canadian High Arctic region from teleseismic receiver function analysis. *Geophysical Journal International*, **152**, 372–391, https://doi.org/10.1046/j.1365-246X.2003.01840.x

Davies, G.R. & Nassichuk, W.W. 1991. Carboniferous and Permian history of the Sverdrup Basin, Arctic Islands. *In*: Trettin, H.P. (ed.) *Geology of the Innuitian Orogen and Arctic Platform of Canada and Greenland*. Geological Survey of Canada, Geology of Canada, **3**, 345–367.

Dawes, P.R. 1997. The Proterozoic Thule Supergroup, Greenland and Canada: history, lithostratigraphy and development. *Geology of Greenland Survey Bulletin*, **174**, 5–12.

Doré, A.G., Lundin, E.R., Kusznir, N.J. & Pascal, C. 2008. Potential mechanisms for the genesis of Cenozoic domal structures on the NE Atlantic margin: pros, cons and some new ideas. *In*: Johnson, H., Doré, T.G., Gatliff, R.W., Holdsworth, R.W., Lundin, E.R. & Ritchie, J.D. (eds) *The Nature and Origin of Compression in Passive Margins*. Geological Society, London, Special Publications, **306**, 1–26, https://doi.org/10.1144/SP306.1

Doré, A.G., Lundin, E.R., Gibbons, A., Sømme, T.O. & Tørudbakken, B.O. 2015. Transform margins of the Arctic: a synthesis and re-evaluation. *In*: Nemčok, M., Rybár, S., Sinha, S.T., Hermeston, S.A. & Ledvényiová, L.A. (eds) *Transform Margins: Development, Controls and Petroleum Systems*. Geological Society, London, Special Publications, **431**, 63–94, https://doi.org/10.1144/SP431.8

Døssing, A., Stemmerik, L., Dahl-Jensen, T. & Schlindwein, V. 2010. Segmentation of the eastern North Greenland oblique-shear margin – regional plate tectonic implications. *Earth and Planetary Science Letters*, **292**, 239–253, https://doi.org/10.1016/j.epsl.2009.12.036

Døssing, A., Jackson, H.R., Matzka, J., Einarsson, I., Rasmussen, T.M., Olesen, A.V. & Brozena, J.M. 2013. On the origin of the Amerasia Basin and the High Arctic Large Igneous Province – results of new aeromagnetic data. *Earth and Planetary Science Letters*, **363**, 219–230, https://doi.org/10.1016/j.epsl.2012.12.013

Døssing, A., Hansen, T.M., Olesen, A.V., Hopper, J.R. & Funck, T. 2014. Gravity inversion predicts the nature of the Amundsen Basin and its continental borderlands near Greenland. *Earth and Planetary Science Letters*, **408**, 132–145, https://doi.org/10.1016/j.epsl.2014.10.011

Embry, A. & Beauchamp, B. 2008. Sverdrup Basin. *In*: Andrew, D.M. (ed.) *Sedimentary Basins of the World: the Sedimentary Basins of the United States and Canada*. Elsevier, Amsterdam, 451–471.

Embry, A.F. 1991. Mesozoic history of the Arctic Islands. *In*: Trettin, H.P. (ed.) *Geology of the Innuitian Orogen and Arctic Platform of Canada and Greenland*. Geological Survey of Canada, Geology of Canada, **3**, 371–433.

Embry, A.F. & Osadetz, K.G. 1988. Stratigraphy and tectonic significance of Cretaceous volcanism in the Queen Elizabeth Islands, Canadian Arctic Archipelago. *Canadian Journal of Earth Sciences*, **25**, 1209–1219, https://doi.org/10.1139/e88-118

Estrada, S. & Henjes-Kunst, F. 2004. Volcanism in the Canadian High Arctic related to the opening of the Arctic Ocean. *Zeitschrift Deutsche Gesellschaft für Geowissenschaften*, **154**, 579–603.

Forsyth, D.A., Mair, J.A. & Fraser, I. 1979. Crustal structure of the central Sverdrup Basin. *Canadian Journal of Earth Sciences*, **16**, 1581–1598, https://doi.org/10.1139/e79-144

Forsyth, D.A., Overton, A., Stephenson, R.A., Embry, A.F., Ricketts, B.D. & Asudeh, I. 1990. *Delineation of Sedimentary Basins Using Seismic Techniques on Canada's Arctic Continental Margin*. Éditions Technip, Paris.

Forsyth, D.A., Argyle, M., Okulitch, A. & Trettin, H.P. 1994. New seismic, magnetic, and gravity constraints on the crustal structure of the Lincoln Sea continent–ocean transition. *Canadian Journal of Earth Sciences*, **31**, 905–918, https://doi.org/10.1139/e94-082

Forsyth, D.A., Asudeh, I., White, D., Jackson, R., Stephenson, R.A., Embry, A.F. & Argyle, M. 1998. Sedimentary basins and basement highs beneath the polar shelf north of Axel Heiberg and Meighen islands. *Bulletin of Canadian Petroleum Geology*, **46**, 12–29.

Funck, T., Jackson, H.R., Dehler, S.A. & Reid, I.D. 2006. A refraction seismic transect from Greenland to Ellesmere Island, Canada: the crustal structure in southern Nares Strait. *Polarforschung*, **74**, 97–112.

Funck, T., Jackson, H.R. & Shimeld, J. 2011. The crustal structure of the Alpha Ridge at the transition to the Canadian Polar Margin: results from a seismic refraction experiment. *Journal of Geophysical Research: Solid Earth*, **116**, B12101, https://doi.org/10.1029/2011JB008411

Gaina, C., Nikishin, A.M. & Petrov, E.I. 2015. Ultraslow spreading, ridge relocation and compressional events in the East Arctic region: a link to the Eurekan orogeny? *Arktos*, **1**, 1–11, https://doi.org/10.1007/s41063-015-0006-8

Gasser, D. 2013. The Caledonides of Greenland, Svalbard and other Arctic areas: status of research and open questions. *In*: Corfu, F., Gasser, D. & Chew, D.M. (eds) *New Perspectives on the Caledonides of Scandinavia and Related Areas*. Geological Society, London, Special Publications, **390**, 93–129, https://doi.org/10.1144/SP390.17

Gee, D.G. 2015. Caledonides of Scandinavia, Greenland, and Svalbard. *In*: Elias, S.A. (ed.) *Reference Module in Earth Systems and Environmental Sciences*. Elsevier, Amsterdam.

Grantz, A., Hart, P.E. & Childers, V.A. 2011. Geology and tectonic development of the Amerasia and Canada Basins, Arctic Ocean. *In*: Spencer, A.M., Embry, A.F., Gautier, D.L., Stoupakova, A.V. & Sørensen, K. (eds) *Arctic Petroleum Geology*. Geological Society, London, Memoirs, **35**, 771–799, https://doi.org/10.1144/M35.50

Grist, A.M. & Zentilli, M. 2006. Preliminary apatite fission track thermal history modelling of the Nares region of eastern Ellesmere Island and northwestern Greenland. *Polarforschung*, **73**, 113–127.

Harrison, J.C. 2006. In search of the Wegener Fault: re-evaluation of strike-slip displacements along and bordering Nares Strait. *Polarforschung*, **74**, 129–160.

Harrison, J.C. & de Freitas, T.A. 2007. *Geology, Agassiz Ice Cap, Ellesmere Island, Nunavut*. Geological Survey of Canada Map, **2104A**.

Heron, P.J., Pysklywec, R.N. & Stephenson, R. 2015. Intraplate orogenesis within accreted and scarred lithosphere: example of the Eurekan Orogeny, Ellesmere Island. *Tectonophysics*, **664**, 202–213, https://doi.org/10.1016/j.tecto.2015.09.011

Hosseinpour, M., Müller, R.D., Williams, S.E. & Whittaker, J.M. 2013. Full-fit reconstruction of the

Labrador Sea and Baffin Bay. *Solid Earth*, **4**, 461–479, https://doi.org/10.5194/se-4-461-2013

Jackson, H.R., Dahl-Jensen, T. & LORITA Working Group 2010. Sedimentary and crustal structure from the Ellesmere Island and Greenland continental shelves onto the Lomonosov Ridge, Arctic Ocean. *Geophysical Journal International*, **182**, 11–35, https://doi.org/10.1111/j.1365-246X.2010.04604.x

Lawver, L.A., Gahagan, L.M. & Norton, I. 2011. Palaeogeographic and tectonic evolution of the Arctic region during the Palaeozoic. *In*: Spencer, A.M., Embry, A.F., Gautier, D.L., Stoupakova, A.V. & Sørensen, K. (eds) *Arctic Petroleum Geology*. Geological Society, London, Memoirs, **35**, 61–77, https://doi.org/10.1144/M35.5

Lebedeva-Ivanova, N.N., Gaina, C., Minakov, A. & Kashubin, S. 2015. A new model of the Arctic crustal thickness from 3D gravity inversion. *Abstract presented at the AGU Fall Meeting*, 14–18 December, 2015, San Francisco, USA.

Lemieux, Y., Hadlari, T. & Simonetti, A. 2011. Detrital zircon geochronology and provenance of Devono-Mississippian strata in the northern Canadian Cordilleran miogeocline. *Canadian Journal of Earth Sciences*, **48**, 515–541, https://doi.org/10.1139/E10-056

Lophaven, S.N., Nielsen, H.B. & Søndergaard, J. 2002. *DACE – A Matlab Kriging Toolbox, version 2.0.* Technical report, 2002, Informatics and Mathematical Modelling, Technical University of Denmark, DTU, Copenhagen.

Nielsen, S.B., Stephenson, R. & Thomsen, E. 2007. Dynamics of Mid-Palaeocene North Atlantic rifting linked with European intra-plate deformations. *Nature*, **450**, 1071–1074, https://doi.org/10.1038/nature06379

Oakey, G.N. & Chalmers, J.A. 2012. A new model for the Paleogene motion of Greenland relative to North America: plate reconstructions of the Davis Strait and Nares Strait regions between Canada and Greenland. *Journal of Geophysical Research*, **117**, https://doi.org/10.1029/2011JB008942

Oakey, G.N. & Stephenson, R. 2008. Crustal structure of the Innuitian region of Arctic Canada and Greenland from gravity modelling: implications for the Palaeogene Eurekan orogen. *Geophysical Journal International*, **173**, 1039–1063, https://doi.org/10.1111/j.1365-246X.2008.03784.x

Oakey, G.N., Hearty, B., Forsberg, R. & Jackson, H.R. 2001. *Gravity anomaly of the Innuitain Region, Canadian and Greenland Arctic*. Geological Survey of Canada Open File Report No. 33934D.

Okulitch, A.V. & Trettin, H.P. 1991. Late Cretaceous–Early Tertiary deformation, Arctic Islands. *In*: Trettin, H.P. (ed.) *Geology of the Innuitian Orogen and Arctic Platform of Canada and Greenland*. Geological Survey of Canada, Geology of Canada, **3**, 467–485.

Pease, V., Drachev, S., Stephenson, R. & Zhang, X. 2014. Arctic lithosphere – a review. *Tectonophysics*, **628**, 1–25, https://doi.org/10.1016/j.tecto.2014.05.033

Petrov, O., Morozov, A. *et al.* 2016. Crustal structure and tectonic model of the Arctic region. *Earth-Science Reviews*, **154**, 29–71, https://doi.org/10.1016/j.earscirev.2015.11.013

Piepjohn, K. & von Gosen, W. 2017. Structural transect through Ellesmere Island (Canadian Arctic): superimposed Palaeozoic Ellesmerian and Cenozoic Eurekan deformation. *In*: Pease, V. & Coakley, B. (eds) *Circum-Arctic Lithosphere Evolution*. Geological Society, London, Special Publications, **460**. First published online May 24, 2017, https://doi.org/10.1144/SP460.5

Piepjohn, K., von Gosen, W., Tessensohn, F. & Saalmann, K. 2008. Ellesmerian fold-and-thrust belt (northeast Ellesmere Island, Nunavut) and its Eurekan overprint. *In*: Mayr, U. (ed.) *Geology of Northeast Ellesmere Island Adjacent to Kane Basin and Nares Strait, Nunavut*. Geological Survey of Canada, Bulletin, **592**, 285–303.

Piepjohn, K., von Gosen, W. *et al.* 2015. Tectonic map of the Ellesmerian and Eurekan deformation belts on Svalbard, North Greenland, and the Queen Elizabeth Islands (Canadian Arctic). *Arktos*, **1**, 1–7, https://doi.org/10.1007/s41063-015-0015-7

Reid, I. & Jackson, H.R. 1997. Crustal structure of northern Baffin Bay: seismic refraction results and tectonic implications. *Journal of Geophysical Research: Solid Earth*, **102**, 523–542, https://doi.org/10.1029/96JB02656

Roest, W.R. & Srivastava, S.P. 1989. Sea-floor spreading in the Labrador Sea: a new reconstruction. *Geology*, **17**, 1000–1003, https://doi.org/10.1130/0091-7613(1989)0172.3.CO;2

Saumur, B.M., Dewing, K. & Williamson, M.-C. 2016. Architecture of the Canadian portion of the High Arctic Large Igneous Province and implications for magmatic Ni–Cu potential. *Canadian Journal of Earth Sciences*, 1–15, https://doi.org/10.1139/cjes-2015-0220

Schiffer, C., Stephenson, R., Oakey, G.N. & Jacobsen, B.H. 2016. The crustal structure of Ellesmere Island, Arctic Canada – teleseismic mapping across a remote intraplate orogenic belt. *Geophysical Journal International*, **204**, 1579–1600, https://doi.org/10.1093/gji/ggv539

Schiffer, C., Tegner, C., Schaeffer, A.J., Pease, V. & Nielsen, S.B. 2017. High Arctic geopotential stress field and implications for geodynamic evolution. *Geological Society, London, Special Publications*, **460**, SP460.6, https://doi.org/10.1144/SP460.6

Srivastava, S.P. 1985. Evolution of the Eurasian Basin and its implications to the motion of Greenland along Nares Strait. *Tectonophysics*, **114**, 29–53, https://doi.org/10.1016/0040-1951(85)90006-X

Steffen, R., Strykowski, G. & Lund, B. 2017. High-resolution Moho model for Greenland from EIGEN-6C4 gravity data. *Tectonophysics*, **706–707**, 206–220, https://doi.org/10.1016/j.tecto.2017.04.014

Stephenson, R., Oakey, G.N., Schiffer, C. & Jacobsen, B.H. 2013. *Ellesmere Island Lithosphere Experiment (ELLITE): Eurekan Basin Inversion and Mountain Building, Ellesmere Island, Nunavut*. Geological Survey of Canada, Current Research, **2013–21**, https://doi.org/10.4095/292859

Stephenson, R., Piepjohn, K., Schiffer, C., von Gosen, W., Oakey, G.N. & Anudu, G. 2017. Integrated crustal-geological cross-section of Ellesmere Island.

In: PEASE, V. & COAKLEY, B. (eds) *Circum-Arctic Lithosphere Evolution*. Geological Society, London, Special Publications, **460**. First published online May 23, 2017, https://doi.org/10.1144/SP460.12

STEPHENSON, R.A. & RICKETTS, B.D. 1989. *Gravity Modelling in the Eurekan Orogen, Canadian Arctic Islands*. Geological Survey of Canada, Current Research, **89-IG**, 225–232.

STEPHENSON, R.A. & RICKETTS, B.D. 1990. Bouguer gravity anomalies and speculations on the regional crustal structure of the Eurekan Orogen, Arctic Canada. *Marine Geology*, **93**, 401–420, https://doi.org/10.1016/0025-3227(90)90095-2

STEPHENSON, R.A., RICKETTS, B.D., CLOETINGH, S.A. & BEEKMAN, F. 1990. Lithosphere folds in the Eurekan orogen, Arctic Canada? *Geology*, **18**, 603–606, https://doi.org/10.1130/0091-7613(1990) 0182.3.CO;2

STEPHENSON, R.A., BOERSTOEL, J., EMBRY, A.F. & RICKETTS, B.D. 1994. Subsidence analysis and tectonic modelling of the Sverdrup Basin. *In*: THURSTON, D.K. & FUJITA, K. (eds) *1992 Proceedings, International Conference on Arctic Margins*, 2–4 September, Anchorage, AK, USA. US Department of the Interior Minerals Management Service.

TEGNER, C., STOREY, M., HOLM, P.M., THORARINSSON, S.B., ZHAO, X., LO, C.-H. & KNUDSEN, M.F. 2011. Magmatism and Eurekan deformation in the High Arctic Large Igneous Province: $^{40}Ar-^{39}Ar$ age of Kap Washington Group volcanics, North Greenland. *Earth and Planetary Science Letters*, **303**, 203–214, https://doi.org/10.1016/j.epsl.2010.12.047

TESSENSOHN, F. & PIEPJOHN, K. 2000. Eocene compressive deformation in Arctic Canada, North Greenland and Svalbard and its plate tectonic causes. *Polarforschung*, **68**, 121–124.

TESSENSOHN, F., JACKSON, R.H. & REID, I.D. 2006. The tectonic evolution of Nares Strait: implications of new data. *Polarforschung*, **74**, 191–198.

TRETTIN, H.P. 1991. Silurian–early Carboniferous deformational phases and associated metamorphism and plutonism, Arctic Island. *In*: TRETTIN, H.P. (ed.) *Geology of the Innuitian Orogen and Arctic Platform of Canada and Greenland*. Geological Survey of Canada, Geology of Canada, **3**, 295–341.